Министерство образования и науки Российской Федерации
Санкт-Петербургский политехнический университет Петра Великого
Институт прикладной математики и механики
Высшая школа теоретической механики

Работа допущена к защите

Директор высшей школы

___________ А. М. Кривцов

«___»_______________20__ г.

ВЫПУСКНАЯ КВАЛИФИКАЦИОННАЯ РАБОТА МАГИСТРА «ТРАДИЦИОННЫЕ И НОВЫЕ МОДЕЛИ ДЛЯ ОЦЕНКИ ДИНАМИЧЕСКОЙ ТЕКУЧЕСТИ»

по направлению 01.04.03 «Механика и математическое моделирование»
по образовательной программе 01.04.03_02 «Механика и математическое моделирование (международная образовательная программа)»

Выполнил
студент гр. 3640103/80201 ____________ К. Гупта

Руководитель
Доцент, к.ф.-м.н. ____________ Е. А. Подольская

Консультант
Научный сотрудник СПбПУ, к.ф.-м.н. ____________ В. А. Братов

Консультант
по нормоконтролю ____________ Е. А. Хайбулова

Санкт-Петербург

2020

Peter the Great St.Petersburg Polytechnic University
Institute of Applied Mathematics and Mechanics
Higher School of Theoretical Mechanics

Work approved

Head of the Higher school

___________ A. M. Krivtsov

«___»_______________20__ г.

GRADUATE QUALIFICATION WORK

«CONVENTIONAL AND NEW MODELS FOR SIMULATION OF DYNAMIC YIELDING»

Subject 01.04.03 «Mechanics and Mathematical Modeling»

Educational program 01.04.03_02 «Mechanics and Mathematical Modeling (international educational program)»

Submitted by
Student of group No.3640103/80201 ____________ K. Gupta

Scientific advisor
Associate Professor, PhD. ____________ E. A. Podolskaya

Work advisor
Scientific researcher of SPbPU, PhD. ____________ V. A. Bratov

Regulatory
advisor ____________ E. A. Khaibulova

Saint Petersburg

2020

ABSTRACT

57 pages, 26 figures, 7 tables, 0 appendices

KEYWORDS: DYNAMIC, FEM, COPPER, HARDENING

The solid materials deform permanently, after applying a force that tends to make a non-reversible change of sample size and shape, to perform the dynamic deformation experiment a Taylor rod- on- anvil impact test experiment is implemented and the simulation is carried out using Finite Element Method (FEM). There are several applied plasticity models for simulation of high strain, high strain rate and high temperature applications has been used like Johnson-Cook, bilinear plasticity, Zerilli-Armstrong model to check the dynamic yielding of specimen along with new models are also employed to check and verify the best desired results, when compared with the experimental data of deformed specimen at different velocities and for different material (Cu - OFHC).It states that previous model results are not up to the mark, and there is a significant deviation in the shape and size of deformed specimen when compared with laboratory and simulation data. The objective of this work is to develop a new deformation model to correctly predict the sample deformation at points distant from the contact surface. To implement a new model, change in yield stress of material is appended in the form internal stress. Accordingly, this modification is carried out using a user subroutine material model code in Fortran language (VUMAT), that resembles the hardening of material.

CONTENTS

List of Figures

List of Tables

NOMENCLATURE

Superscripts

pl	Plastic
el	Elastic

Notation

C_{ijkl}	Elasticity tensor
δ_{ij}	Kronecker delta
c_p	Specific Heat
Δ	Increment
E	Young's Modulus
e_{ij}	Deviatoric Strain
ε_{ij}	Strain
$G(N)$	Shear Modulus
$K(B)$	Bulk Modulus
ν	Poisson's ratio
σ_{ij}	Stress
η	Viscosity Constant
μ	Spring Constant
σ_y	Yield stress
t	Time
T	Temperature
T_{melt}	Melting temperature
T_{ref}	Reference temperature
V	Velocity

ρ	Density
σ_H	Hydrostatic stress
$\dot{\varepsilon}_p$	Plastic Strain rate
ε_p	Equivalent plastic strain
J	Hardening parameter
h	Plastic hardening
τ	Relaxation time
$\cdot$	Dot above rate

INTRODUCTION

1.1 Background and Motivation

To investigate the dynamic deformation of materials, several research has been fulfilled and some are in progress, as it possess numerous of mechanical application like crash, impact and ballistic testing [1]. Elastic and plastic stress states define a major role to define the dynamic yielding of material and strain increment. The stress state in the yield surface is elastic, once the stress state lies on the surface of material and reached its yield point, in that case material shows plastic behavior. If the material continuously deformed the stress state remains on yield surface along with change in shape and size of material [2]. There are various different yield surfaces known in engineering, to define the constitutive model of material and to evaluate the process of deformation in finite element analysis (FEA). The best yield surface model should be selected that should predicts the correct different material behavior, like isotropic and kinematic strain hardening, yielding stress.

In literature, several models of plastic deformation of material and yield criterion have been used by many authors to define the dynamic deformation of material Wilkins [3], Eakins, Thadhani [4] but all these models have limitation. Among those classic von Mises criterion was actively used for isotropic material [5-8]. This is the most widely used yield criterion model till the last century, it is due to inability of this model to predict the high rate deformation of order 10^3 s-1 to 10^4 s-1. At the same time, several other widely used models are discussed and compared among each other to have the best dynamic deformation results.

During model simulation comparison, there is a noticeable error in models that are included in FEM software, that motivates to implement a new model with best possible solution with a smaller number of model coefficients.

This thesis mainly focusses on implementing a new model by accepting all the drawbacks of conventional model.

1.2 Scope of Thesis

The main objective of this thesis is to compare numerical results of the proposed models that are included in commercial FEM codes (Abaqus, Ansys) with the laboratory performed experimental data. A theoretical review will be fulfilled to choose the model which define the best material behavior by predicting precise shape and size of deformed material with experimental results.

In this thesis, there will be total four different FEM models of simulation on dynamic deformation will be performed using rod on anvil impact test with the velocity (83 m/s), while using OFHC grade rod copper of length (76.2 mm) and diameter (19.05 mm) for both the numerical analyses and experimental study. The numerical simulation is performed at two different FEM software Ansys Workbench and Abaqus. According to the aim of thesis the new model is implemented to Abaqus software via the user material subroutine (VUMAT) with all the necessary parameters and included dynamic yield stress under changeable parameter of strain and strain rate (for isotropic material) to predict the best solution.

1.3 Outline of the Thesis

This thesis begins with an elementary chapter (Chapter 2). A literature study on impact tests, particularly Taylor impact test, is described. The objective and motivation of this research is briefly discussed, and all other chapters is followed accordingly.

Chapter 3, the finite element simulation is performed on the four different material models, simultaneously results of experiments for OFHC copper material are presented and then comparison of the simulation results with the experimental data is accomplished.

Chapter 4 presents the new model implementation, how the change in the dynamic yield stress impacted material during simulation, its significant characteristics during analyses.

Chapter 5 the results and discussion of the FEA of new and conventional model is discuss along with transient deformation of profile during numerical simulation.

Chapter 6 contains the conclusion of the thesis and suggestions for future work.

CHAPTER 1. THEORETICAL BACKGROUND

As per record, a lot of information available about the different constitutive models and their execution in FEM software. This thesis is focused on the research work related to implementation of constitutive models of dynamic deformation process by means of ABAQUS software and the comparison of the simulation results of conventional and new model with the experimental results.

A constitutive equation is a junction between two quantities i.e. kinetic and kinematic these quantities are specific and tells the response of material externally when forces are applied.

The stress-strain is a constitutive equation originated from the Hooke's law: It states stresses inside the body is directionally proportional to the strain, when a body is subjected to external loading. [9]

$$\sigma = E\varepsilon (1.1)$$

The external load is applied on a body and due to which deformation happens which is generally in normal direction and in tangential direction, defining numerically using stress tensor as:

$$\sigma_{ij} = C_{ijkl}\varepsilon_{kl} \approx \varepsilon_{ij} = S_{ijkl}\sigma_{kl} (1.2)$$

where C is the elasticity tensor and S is the compliance tensor.

Solid-state deformations: Several forms of deformations in materials is possible:[10]

Elastic: The material retrieves its initial shape after getting deformation.

Inelastic: In this case material shows almost elastic properties, but the force applied include resistive force that is time dependent. Examples are like metals and ceramics that shows this characteristic in general it is very small till the time friction generates. For example, machine produces a large vibrations and stresses.

Viscoelastic: This plays a major role to define the solid-state deformation as if time-dependent resistive is large and taken into account.

Plastic: This is a common behavior perceived in materials that after applying a force material does not come to its original shape and size as the stress reaches to yield point and if there is any more increase in stress it leads to a permanent deformation in material.

Hyperelastic: In this deformation there accounts the displacement in material due to strain energy density function.

When several equations are defined to get a response of material under a specified load, then those models are termed as material model. The models introduced in this review are valid for metals mainly focused on large strains, high strain rates and high temperatures. In this thesis Von- Mises, Johnson-Cook, Zerilli-Armstrong, Steinberg Guinan and New material model is implemented and will also be discussed both numerically and analytically along with a verification of results with experimental data.

1.1 Stress Tensor

This tensor comprises of nine components σ_{ij} that completely define the state of stress at a point inside a material in the deformed state, placement, or configuration. The tensor relates a unit-length direction vector m to the traction vector T(m) across an imaginary surface perpendicular to m [11]:

$T^{(m)} = m.\sigma$ or $T_j^{(m)} = \sigma_{ij} n_i$.

where,

$$\sigma = \begin{bmatrix} \sigma_{11} & \sigma_{12} & \sigma_{13} \\ \sigma_{21} & \sigma_{22} & \sigma_{23} \\ \sigma_{31} & \sigma_{30} & \sigma_{33} \end{bmatrix} \equiv \begin{bmatrix} \sigma_{xx} & \sigma_{xy} & \sigma_{xz} \\ \sigma_{yx} & \sigma_{yy} & \sigma_{yz} \\ \sigma_{zx} & \sigma_{zy} & \sigma_{zz} \end{bmatrix}$$

1.2 Hydrostatic and deviatoric components

Mainly, the stress tensor can be separated into two components. One component is a hydrostatic or dilatational stress that acts to change the volume of the material only; the other is the deviatoric stress that acts to change the shape only.

$$\begin{bmatrix} \sigma_{11} & \sigma_{12} & \sigma_{13} \\ \sigma_{21} & \sigma_{22} & \sigma_{23} \\ \sigma_{31} & \sigma_{30} & \sigma_{33} \end{bmatrix} = \begin{bmatrix} \sigma_H & 0 & 0 \\ 0 & \sigma_H & 0 \\ 0 & 0 & \sigma_H \end{bmatrix} + \begin{bmatrix} \sigma_{11} - \sigma_H & \sigma_{12} & \sigma_{13} \\ \sigma_{21} & \sigma_{22} - \sigma_H & \sigma_{23} \\ \sigma_{31} & \sigma_{30} & \sigma_{33} - \sigma_H \end{bmatrix}$$

where the hydrostatic stress is given by $\sigma_H = \frac{1}{3}(\sigma_1 + \sigma_2 + \sigma_3)$

1.3 Linear Elasticity

Material that return to its original shape and size after loading and unloading of forces. [12]. It can therefore be classified as being non-dissipative. If a material is subjected to small strains, they generally show this characteristic and their behavior is easily analyzed through linear elasticity. In this behavior of material stress and strain are proportional to each other and can be generalized by the statement of Hooke's law, termed as [13]:

$$\sigma_{ij} = C_{ijkl}\varepsilon_{kl}(1.3.1)$$

where ε_{kl} is known as elastic strain tensor and $C_{ijkl}$is termed as 4th order tensor of elastic components.

In the study of mechanical properties of material, "isotropic" material shows the unique values of properties in all direction and does not depend on the direction, once the load is acted on the material [14]. The elasticity tensor for isotropy material consists of two parameters know as Lame's constant, λ and μ. Whereas μ is known as shear modulus of the material and the stress tensor along with these two parameters is termed as following:

$$\sigma_{ij} = \lambda\varepsilon_{kk}\delta_{ij} + 2N\varepsilon_{ij}(1.3.2)$$

The constitutive equation is written in terms of deviatoric and mean stress. This equation is important when metal plasticity is included so, the bulk modulus is termed as following:

$$B = \frac{\sigma_{ij}}{3\varepsilon_{kk}} = \frac{\sigma_d}{\varepsilon_{kk}}(1.3.3)$$

The elastic deviatoric constitutive formulation is thus:

$$\sigma_{ij} = S_{ij} + \sigma_d\delta_{ij} = 2Ne_{ij} + B\varepsilon_{kk}\delta_{ij}(1.3.4)$$

1.4 Metal Plasticity

As discussed above, plasticity is a general phenomenon that exits in material, that mainly occurs when the applied stress reaches to yield point. The name plastic comes from a Greek word, πλαστική, which means “to shape" [14]. In this context it is applied to ductile metals as shape of material changes under an adequate amount of load in supplied. In this deformation deviatoric stress and strains are accounted to describe the plasticity behavior and the deformation happens due to slip or shear in particles and accordingly deformation does not depend on hydrostatic stress [13].

Incremental plasticity theory assumes that the rate of deformation can be described as the summation of an elastic and a plastic component [13,14,15]. The total strain rate is termed as following:

$$\dot{\varepsilon} = \dot{\varepsilon}_{ij}^{e} + \dot{\varepsilon}_{ij}^{pl} \quad (1.4.1)$$

where $\dot{\varepsilon}_{ij}^{e}$ is termed as elastic component and $\dot{\varepsilon}_{ij}^{pl}$ is known as plastic component. The simplest form after integration is defined as [15]:

$$\varepsilon = \varepsilon_{ij}^{e} + \varepsilon_{ij}^{pl} \quad (1.4.2)$$

So, as to distinguish plasticity models, three relations are generally divided that shows the evolution of elastic and plastic response:

·*Yield surface:* defines the state of stress and when yielding occurs.

·*Flow rule:* defines the direction of the inelastic deformation in metal plasticity.

·*Hardening law:* defines the variation of material strength, how the yield varies with plastic deformation.

1.4.1 Yield Surface

The yield surface defines the state of stress and calculate both the elastic and plastic behavior of material once the plasticity begins. When the stress state lies on the surface the material is said to have reached its yield point or defines an initial yield point. The stress taken to define the yield point is 0.2% value of plastic strain produced.

We can write the equation of yield surface as a function as following [13,15]:

$$f\left(\sigma_{ij}, \varepsilon_{ij}^{pl}, T, k\right) = 0(1.4.1.1)$$

It is shown that yield surface is a function of stress, plastic strain rate, temperature and one or more hardening parameters. If the function f for stress state is less than zero, it shows material behaves elastically and within elastic limits and in case if f is zero material shows both elastic and plastic behavior. Also, from the above definition, stress state is never be outside the yield surface.

The yield function is usually expressed in terms of a three principal stresses $\sigma_1, \sigma_2, \sigma_3$, when there is an assumption that initial yield surface is isotropic. If we add another assumption that yield function is not a function of hydrostatic pressure, then the final yield function can be written in the following form [13]:

$$f_1(J2, J3) = 0(1.4.1.2)$$

where $J2 = \frac{1}{2} S_{ij} S_{ij}$and $J3 = \frac{1}{3} S_{ij} S_{jk} S_{kl}$ are the 2nd and 3rd invariants of the deviatoric stress tensor.

According to von Mises or Distortion Energy theory, when von Mises induced in the material is either greater than or equal to the yield stress of simple tension test material distortion occurs i.e. yielding in a material takes place when shear distortion energy of the multi-axial stress state is either greater than or equal to maximum shear distortion energy at yield point under actual system (simple tension) [13, 16, 17], It is shown as :

$$\sigma_y = \sqrt{\frac{(\sigma_1 - \sigma_2)^2 + (\sigma_2 - \sigma_3)^2 + (\sigma_3 - \sigma_1)^2}{2}} (1.4.1.3)$$

This can be re-written in terms of the 2nd invariant of the shear stress tensor (called J2 flow theory):

$$\sigma_y = \sqrt{\frac{3}{2} S_{ij} S_{ij}} (1.4.1.4)$$

This yield stress is a scalar quantity which is known as the Mises equivalent stress, q. i.e.,

$$q = \sqrt{\frac{3}{2} S_{ij} S_{ij}} (1.4.1.5)$$

The graphical view of von Mises stress is shown in the Haigh-Westergard principal stress space [13]. To show the 3D stress state the three principal stresses is represented as a vector.

The Distortion energy theory can be viewed as circular cylinder with its centerline accounting $\sigma_1 = \sigma_2 = \sigma_3$ stress line in principal stress space.

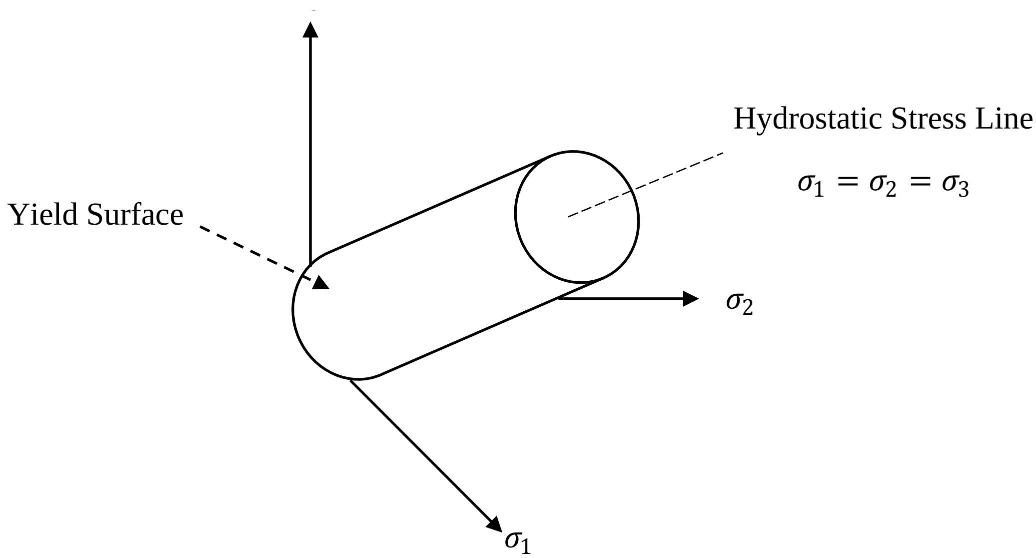

Figure 1: von Mises criteria in Haigh-Westergard principal stress space [13]

To represent von Mises yield criteria in the Pi plane, the plane is defined which is normal to the hydrostatic stress line and passing through the origin. If the principal stress axes are projected on the Pi plane then their values are $\sqrt{\frac{2}{3}}$ of their nominal values [13, 18].

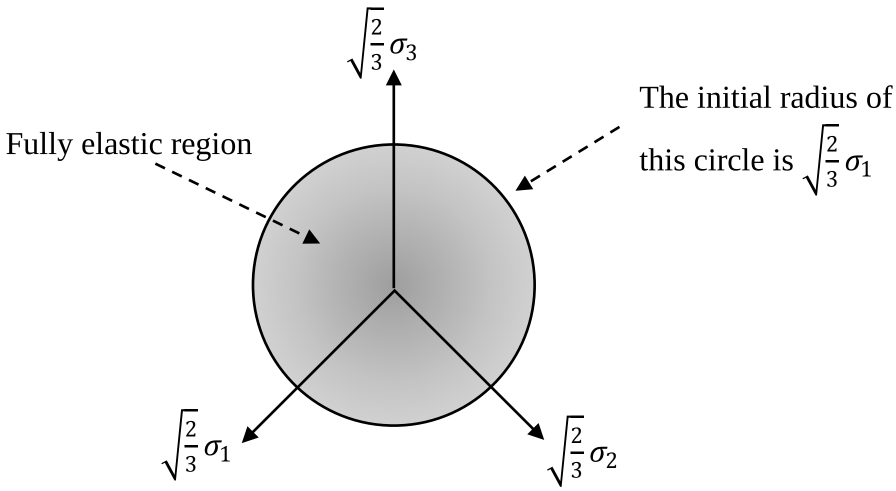

Figure 2: von Mises yield criteria in the Pi plane [13, 18]

1.4.2 Flow Rule

This rule mainly describes the plastic behavior and the direction of plastic deformation through the direction of plastic strain. According to Saint-Venant [18] in 1870 stated that there is a correlation between the directions of the principal axes of strain increment tensor and axes of the stress tensor as they coincided with each other. Also, Lévy and Mises formulated a flow rule that relates the total strain increments to the total shear stresses known as the Lévy-Mises equations [18]:

$$d\varepsilon_{ij} = S_{ij}d\lambda, \text{ d}\lambda \text{ is a positive scalar, changes with loading history}$$

According to this rule the strain generated is due to plastic strain, without any elastic strain accounted. Well know Prandtl and Reuss makes necessary modification in this rule and extended to involve both elastic and plastic strain the overall relations are known as the Prandtl-Reuss equations [18].

$$d\varepsilon_{ij}^{pl} = S_{ij}d\lambda (1.4.2.1)$$

According to von Mises the plastic strain increments can be obtained from a plastic flow potential, which is shown as following [13]:

$$d\varepsilon_{ij}^{pl} = d\lambda \frac{\partial g}{\partial \sigma_{ij}} (1.4.2.2)$$

According to associated flow rule, if plastic flow potential is equal to the yield function, then yield function is linked with the plastic strain increments. If we differentiate the von Mises yield function with respect to the total stress, then the Prandtl-Reuss equation is the flow rule associated with the von Mises yield function [13]. The below equation is to find the plastic strain increment components and simultaneously scalar value dλ can be calculated.

$$\frac{1}{2}d\varepsilon_{ij}^{pl}\left(d\varepsilon_{ij}^{pl}\right)=\frac{1}{2}d\varepsilon_{ij}^{pl}\left(S_{ij}d\lambda\right)$$
$$=\frac{1}{2}S_{ij}\left(S_{ij}d\lambda^{2}\right)(1.4.2.3)$$

By using the definition of the Mises equivalent stress, (q) and the equivalent plastic strain increment is well-defined as:

$$d\varepsilon_{ij}^{pl}=\sqrt{\frac{2}{3}d\varepsilon_{ij}^{pl}d\varepsilon_{ij}^{pl}}(1.4.2.4)$$

equation can be solved for dλ and the plastic strain increment is:

$$d\varepsilon_{ij}^{pl}=\frac{3d\varepsilon_{ij}^{pl}}{2q}S_{ij}(1.4.2.5)$$

From the above defined equation, $\sqrt{\frac{2}{3}}$ is the factor in equivalent plastic strain increment and $\sqrt{3}$ factor in the Mises equivalent stress (q) are chosen and provided with uniaxial tension experiments [17].

1.4.3 Hardening Rule

This rule deals with the variation of material strength. So, as to get the hardening generated inside the material after yield occurs, the applied stress should continuously increase so as to get plastic deformation. If the stress is constant no further plastic deformation occurs. There are three general models for hardening [13,14]:

·**Isotropic:** the center of the yield surface is fixed while the surface expands uniformly (Figure 3 a)

·**Kinematic:** the yield surface translates without any change of shape (Figure 3 b).

·**Combined:** involves both types of hardening i.e. expansion and translation of yield surface (Figure 3 c).

To explain all these models, let's take a uniaxial loading case, we assume that the sample is loaded till yield point. In the figure (3a) the small diameter circle shows the von Mises yield surface that corresponds to the loading state at stress σ. If we are in elastic region, we will be inside the small circle, for elasto-plasto region we will be on the yield surface, but we can't go beyond it. If the sample is loaded with the stress $\sigma + \partial\sigma$, then we will check how yield surface evolves under isotropic hardening, as it characterizes by uniform yield surface expansion. At stress $\sigma + \partial\sigma$, bigger circle shows the yield surface it results in the symmetry of tension and compression behavior. In kinematic hardening, shift of yield surface starts without any change in size/shape takes place and the new yield surface is shown in figure (3b) $\sigma + \partial\sigma$ as we gain some strength in tension, we lose strength in compression, this asymmetric behavior is known as the Bauschinger effect.

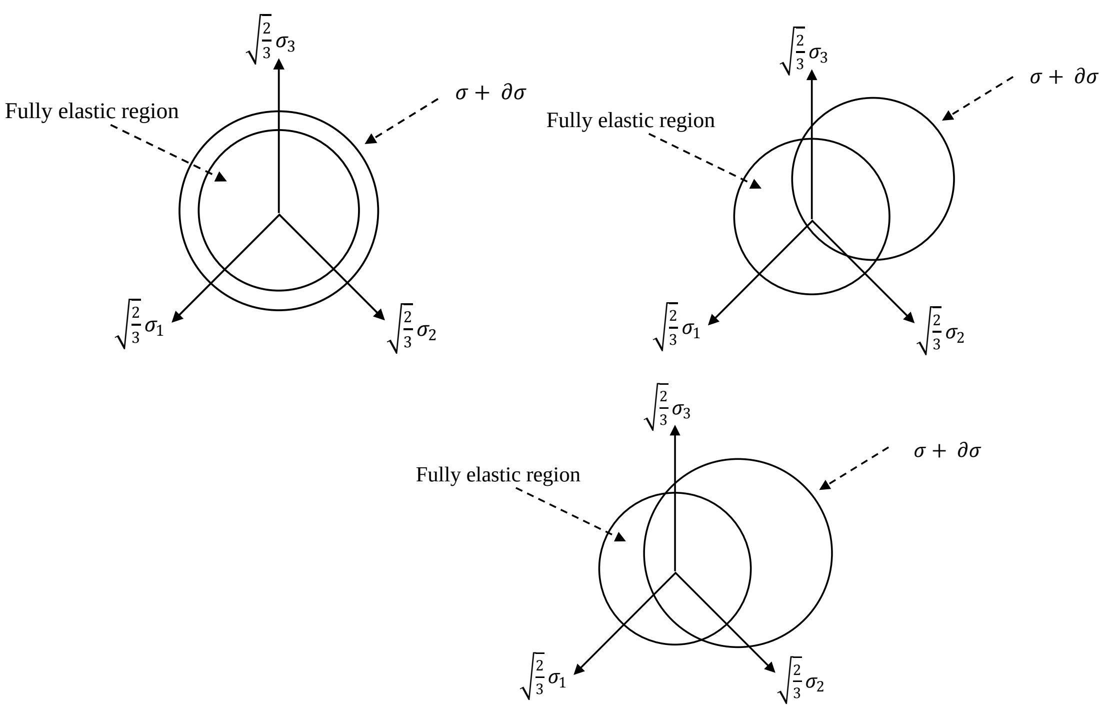

Figure 3: Isotropic(a), Kinematic(b), and Combined(c) Hardening [13,14]

Metals generally shows discussed above hardening behavior; therefore, the stress-strain path can be shown as a function of equivalent plastic strain increment [13]:

1.5 Specific Forms of the Equivalent Flow stress

So as to know which form of equivalent flow stress ($\overline{\sigma}$) is needed to define the Mises yield criteria, loading condition and type of material is important.

If a material is deformed at low strain rate and temperature, then we can use power law flow stress equation shown as Ludwik (1909) [19, 20]:

$$\overline{e}^{pl} = \int \sqrt{\frac{2}{3} d\varepsilon_{ij}^{pl} d\varepsilon_{ij}^{pl}} \ (1.5.1)$$

A good flow stress equation should include parameters like strain rate, temperature, strain and strain rate history and its strain hardening behavior [13]. In reality to include all is hard so in general strain, strain rate and temperature dependence are included.

Flow stress are generally discussed in two ways: first is phenomenological and second is dislocation-mechanics-based. The first approach takes into account the changes with plastic strain, temperature and strain rate. This approach provides the good result when strain hardening factor is accounted as we can also accomplish the magnitude of the curve experimentally, when state history in included in the plastic strain [19]. If we also include the internal state of material during deformation provides the best result. The material models to be described fall into the different categories of flow stress equations. It can also be divided into two categories i.e. rate-independent plasticity model like Von-Mises or J2 plasticity and rate dependent models like Isotropic hardening (dislocation structure)[22], Johnson-Cook [25], models is of the phenomenological type, while the Steinberg Guinan[23], Zerilli Armstrong [24] is of the dislocation-mechanics-based type.

1.5.1 von Mises

The von Mises yield theory states that the deformation in material starts, when the second invariant of deviatoric stress J2 reaches a critical value. This theory best applies to ductile materials, such as some metals. Before deformation, any response of material can be expected a linear and nonlinear elastic behavior.

In the below case, we assume material deformation starts when von Mises stress are either equal or greater than yield strength, σ_y . This theory can predict the deformation of materials under complex loading.

This theory does not depend on the first stress invariant, I_1 as discussed, this theory best applies to ductile materials and during the start of deformation process material does not depend on the volumetric component of the stress tensor.

Mathematical expression is as followed [26]:

$$J2 = l^2 \quad (1.5.1.1)$$

where l is termed as yield stress. The value of this stress during shear is (√3) times less than tensile stress in tension.

$l = \frac{\sigma_y}{\sqrt{3}}$ where σ_y is termed as tensile yield strength. If we evaluate von Mises stress as yield strength and merge equation, then von Mises can be termed as:

$$\sigma_y = \sigma_v = \sqrt{3J2} \quad (1.5.1.2)$$

For 2D Planar Case:

$$\sigma_v = \sqrt{\frac{(\sigma_1 - \sigma_2)^2 + (\sigma_2 - \sigma_3)^2 + (\sigma_3 - \sigma_1)^2}{2}} \quad (1.5.1.3)$$

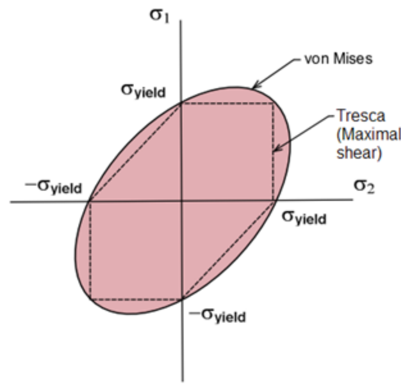

Figure 4: von Mises yield criterion in 2D Planar loading [26]

$\sigma_v = \sqrt{\frac{3}{2} S_{ij} S_{ij}}$, where S_{ij} are the components of the stress deviator tensor

If we take the case of **principal plane stress**, σ_3= 0 and $\sigma_{12} = \sigma_{23} = \sigma_{31} = 0$, the von Mises criterion termed as:

$$\sigma_1{}^2 - \sigma_1 \sigma_2 + \sigma_2{}^2 = \sigma_y = 3l^2 \quad (1.5.1.4)$$

1.5.2 Johnson-Cook

In the late 20th century i.e. in 1983 Johnson and Cook [25] proposed a material model that is applied when materials are under large strains, high strain rates and high temperatures.

This model is popular and widely used due to the relative ease of obtaining its constants, and easy implementation of its variables, parameters or constant. If different models for some individual materials are applied, they provide relatively good results, but those material models are highly complicated when to obtain parameters or constant and often consume more time if we compare Johnson-cook model.

The Johnson-Cook material model states the product of the three main relations. These material relations are function of the multiplicative effects of the strain, strain rate and temperature [28]. There is no representation of thermal or strain rate history effects. The von Mises equivalent flow stress can be written as [25]:

$$\sigma_y(\varepsilon_p, \dot{\varepsilon}_p, T) = [A + B(\varepsilon_p)^n][1 + C\, ln(\dot{\varepsilon}_p^*)][1 - (T^*)^m] \quad (1.5.2.1)$$

where ε_p, $\dot{\varepsilon}_p$ are plastic strain and strain-rate, and A, B, C, n, m are material constants.

The strain-rate and temperature equation are termed as:

$$\dot{\varepsilon}_p^* = \frac{\dot{\varepsilon}_p}{\dot{\varepsilon}_{p0}} \quad \text{and} \quad T^* = \frac{(T - T_0)}{(T_m - T_0)}$$

where $\dot{\varepsilon}_{p0}$ is effective strain rate to determine yield of material and some hardening parameters are A,B, n along with $\dot{\varepsilon}_p^*$ a non-dimensional parameter [40]. T_0, T_m is a reference and melting temperature. For conditions where T^*< 0, we take m = 0.

1.5.3 Steinberg-Guinan

The Steinberg-Guinan strength model popularly used for the high-strain-rate regime and it is further implemented to low strain-rates and bcc materials. This constitutive model results in good prediction of the final deformed state of the impacted samples at low velocities, as well as the transient deformation state is up-to mark. The flow stress of this model is stated as [23]

$$\sigma_y(\varepsilon_p, \dot{\varepsilon}_p, T) = [\sigma_\alpha f(\varepsilon_p) + \sigma_t(\dot{\varepsilon}_p, T)]; \frac{\mu(p,T)}{\mu_0}; \sigma_\alpha f \leq \sigma_{\max} \text{ and } \sigma_t \leq \sigma_p \qquad (1.5.3.1)$$

where σ_α is a component that does not involve either change in temperature or heat, $f(\varepsilon_p)$ is a function informs about strain hardening, σ_t thermal incubated parameter, $\mu(p, T)$ is shear modulus as a function of pressure and temperature, and μ_0 is standard shear modulus. σ_{max} saturation value of σ_α. Peierls stress (σ_p) is a thermal stress parameter.

The strain hardening function (f) form is as follows:

$$f(\varepsilon_p) = [1 + \beta(\varepsilon_p + \varepsilon_p i]^n \qquad (1.5.3.2)$$

In this equation, work hardening parameters are β and n , and initial equivalent plastic strain $\varepsilon_p i$.

σ_t thermal incubated parameter is carried out using a bisection algorithm from the below equation [21].

$$\dot{\varepsilon}_p = [\frac{1}{C_1} exp[\frac{2U_k}{k_b T}(1 - \frac{\sigma_t}{\sigma_p})^2] + \frac{C_2}{\sigma_t}]^{-1}; \sigma_t \leq \sigma_p \qquad (1.5.3.3)$$

where $\frac{2U_k}{k_b T}$ is the energy to form a kink-pair in a dislocation segment of length L_d, k_b is the Boltzmann constant, σ_p is the Peierls stress. The constants C_1, C_2 are given by the relations

$$C_1 = \frac{\rho_d L_d a b^2 v}{2\omega^2}; C_2 = \frac{D}{\rho_d b^2}$$

Here dislocation, density and length are defined as ρ_d, L_d, distance between Peierls valleys is a, b is defined as Burgers vector, Debye frequency (v), width of a kink loop (ω), drag coefficient is D.

1.5.4 Zerilli-Armstrong

The key point to use Zerilli-Armstrong [24] models is to describe individual material responses during the simulation of Taylor impact tests. In this particular material model relations are totally focused on thermal effects and analysis along with that the effects of strain, strain rate hardening and thermal softening of material. This models also include internal grain structure and size of material.

The constitutive relation and equations are based on dislocation-mechanics. Major focus is on the set of each material structure type (BCC, FCC etc.) and having its own constitutive equation based on that materials particular rate-controlling mechanism [28]. Due to this main feature in this material model, particular temperature dependent strain rate effects are calculated for different types of material. Zerilli and Armstrong [24] state that the simulation of the Taylor test provides a decent test of the material model. This is particularly valid if the material parameters were not obtained from the Taylor test but from quasi-static material tests.

$$\sigma_y(\varepsilon_p, \dot{\varepsilon}_p, T) = \sigma_\alpha + B\, exp(-\beta T) + B_0\sqrt{\varepsilon_p}\, exp(-\alpha T) \quad (1.5.4.1)$$

In this model, σ_α flow stress component is given as:

$$\sigma_\alpha = \sigma_g + \frac{k_h}{\sqrt{l}} + K(1.5.4.2)$$

where σ_g influences in the initial dislocation density, microstructural stress intensity (k_h), average grain diameter (l), K is zero for fcc materials, material constants (B,B_0).

In the thermally terms, exponents α and β in their broad forms are as follows:

$$\alpha = \alpha_0 - \alpha_1 \, ln(\dot{\varepsilon}_p); \beta = \beta_0 - \beta_1 \, ln(\dot{\varepsilon}_p) \quad (1.5.4.3)$$

where $\alpha_0, \alpha_1, \beta_0, \beta_1$ directly depends on the material like (fcc, bcc, hcp, alloys).

1.6 Taylor Test

In the last 20th century 1940's, Taylor [41, 42] used a flat-ended rod that is impacted to a flat rigid target i.e. anvil to determine the dynamic yield stress of the impacted rod. This is one of the easiest and best method to achieve high strain rates in material testing, typically in the range $10^4 – 10^6$ s-1. Once the rod is impacted on anvil the front end deforms plastically and rear end does not deform. A large amount of stresses is generated at the front end of rod till elastic limit is reached and after impact the rod bounce back towards free end. The major deformation in rod includes the change in axial and radial position as axial position reduces and radial position increases symmetrically [43].

This test is conducted to obtain material strength parameters for high strain rate models and there are wide range of techniques to optimize these coefficients by performing numerical analysis in FEM software for the Taylor test [44]. This test is also used to validate high strain rate material models by comparing the simulation of the test to the experimental results this technique is simple and cost effective to procure new plasticity model. The coefficients and constant used in simulations are those determined using lower strain rate material testing techniques and then the Taylor test simulation is used to test the verification of the material model to high strain rates [23,24,25,26].

This experimental method is connected with dynamic deformation of cylindrical samples on a rigid wall (Fig. 5)

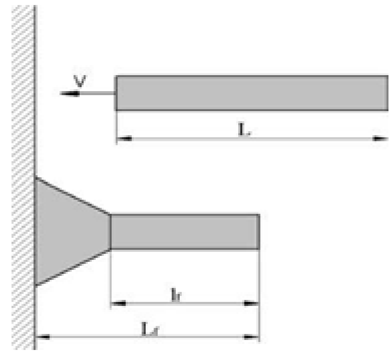

Figure 5: Illustration of the idea of the Taylor impact test [43]

The experiment performed in laboratory results in a plastically deformed specimen and deformation occurs at the impacted end. So, as to calculate the dynamic yield stress all change in dimension is needed. This can be executed by using simple equation:

$$\sigma = \frac{\frac{1}{2}\rho V^2\left(1-\frac{l_f}{L}\right)}{(1-\frac{L_f}{L})\,ln(\frac{L}{l_f})}\,(1.6.1)$$

To calculate the dynamic yield stress, we only need information about the impact velocity V, the length of the undeformed part of sample l_f, and L, L_f – the initial and final length of the sample, respectively.

There is not so much information is available once we start modelling in simulation software, but the available information can classify the material. As we need more information apart from dynamic yield stress. This can be formulated either from constitutive equations or simply formulating your own constitutive material model.

Velocity (m/s)	Initial diameter, d_0 (mm)	Initial length, l_0	Final diameter, d_f	Final length, l_f
83	19.1	75.1	23.6	70.3
205	18.9	75.0	36.6	54.5

Table 1: Impact test experimental data [4]

Impact experiments on OFE copper were performed at 83 and 205 m/s to showcase the phase in deformation response. The lengths and diameters of the initial and final impacted rods from each experiment are listed in Table 1, where the final diameter refers to that of impact end of rod [4].

1.7 Summary of Chapter 1

The background and theory of all conventional model like Steinberg-Guinan [23], Zerilli-Armstrong [24], Johnson-Cook [25], and Von-mises [26], are discussed briefly in this chapter. The linear elastic component of the material model is discussed followed by the plasticity component. The discussion of the plasticity component involved the form and function of the yield surface, flow rule and hardening law which together define the plasticity component. All models detailed formulation is discussed so that it is easy to understand during implementing their parameters in FEM software

The definition and applicability of the Taylor test is discussed briefly along with that experimental data is taken from one the renowned research paper [4]. This data is our base to discuss all the numerically implemented material model in FEM software in the following chapters it is discussed and used widely. Once comparing of simulated data of material models is analyzed with the experimental data it shows the applicability of different material models and tell us about their exactness of predicting results.

CHAPTER 2. METHODS

In this chapter, we are going to discuss more about conventional plasticity methods and their implementation in Finite element software like Abaqus and Ansys. In the numerical modelling of Taylor Test, a 2D planar problem is performed, using the axial symmetry of material with a mesh size of 1mm. Rod is 76.2 mm long and 19.05 mm wide [4].

Models like Von-Mises [26], Johnson Cook [25], Steinberg Guinan [23] and Zerilli Armstrong [24] are discussed with their applied parameters on same yield strength so, as to compare their results with experimental data of similar impact test and taking into account the comparison statistics. A brief summary is discussed at the end of this chapter in which all the results of material model is concluded.

2.1 von Mises Plasticity Model

The von Mises yield criterion, which has been used to describe the dynamic characteristics of material deformation was actively used in the middle of the last century, this plasticity provides best results when applied to ductile materials i.e. on metals. This theory is termed as von Mises stress $\sigma_v$which is a scalar value calculated from the Cauchy stress tensor. The material start deforming when the von mises stress either reached to yield strength σ_y of material or once gets increased. This model predicts the plastic deformation of material at high velocity impact/loadings as this independent of first stress Invariant, the yield stress of material does not directly relate with hydrostatic component of stress tensor [26].

This model is implemented in FEM software with the following parameters for OFHC Cu at 83 m/s. After applying following parameters in FEM software, the final deformed profile is shown along with a graph of final deformed sample profile including change in axial position

Table 2: Von-Mises Simulation Parameters (Author)

No	Constant	Value	Unit
1	E – Young’s modulus	124	Gpa
2	ν - Poisson’s ratio	0.34	-

3	Density	8960	Kg/m^3
4	Bulk modulus	129	Gpa
5	Shear modulus	46	Gpa
6	Stress	300	Mpa
7	Strain	0.2	-

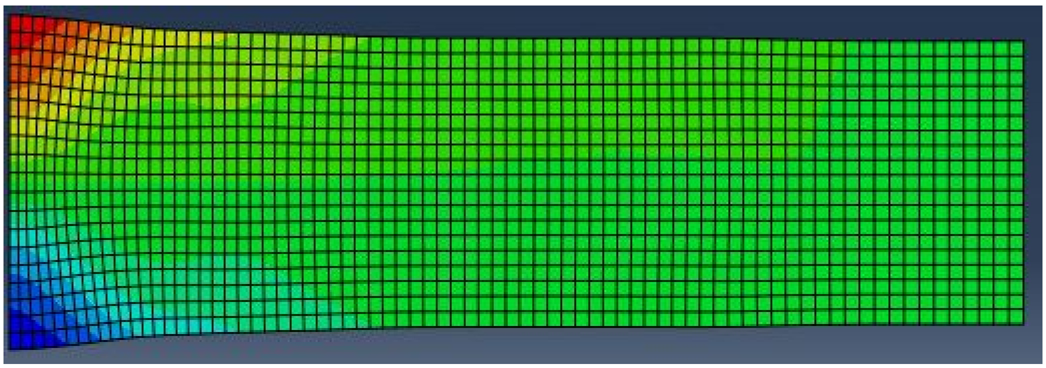

Figure 6: von Mises Deformed Profile (Author)

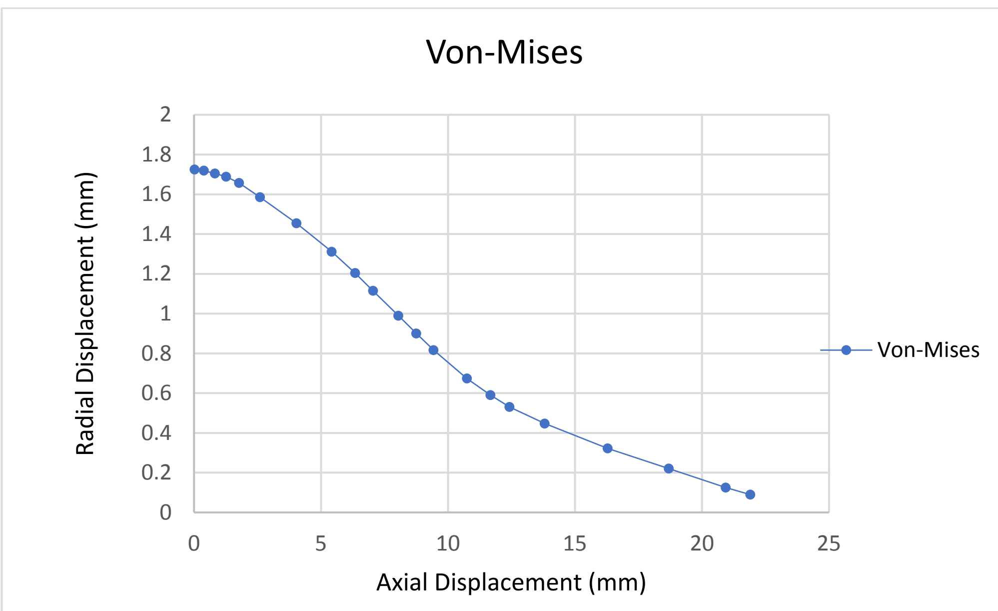

Figure 7: von Mises Profile Graph with deformation (Author)

2.2 Johnson-Cook Plasticity Model

Johnson-Cook is a particular type of isotropic hardening model so as to characterize the dynamic behavior of materials subjected to high strain and strain rates along with temperature. It is suitable for high-strain-rate deformation of many materials, including most metals. The equivalent von mises flow stress of this model is broadly divided into multiplication of 3 sections, first section defines the stress-strain relation, second defines the strain rate and third shows the dependency with temperature. It is broadly used in simulations due to its simplicity and uncomplicated way of finding its constant. The variables implemented in this model is available in almost all simulation software's.

In our thesis we have also implemented this model in FEM software with the following parameters for OFHC Cu at 83 m/s. Following results in both axial and radial directions are observed after implementation.

Table 3: Johnson-Cook Simulation Parameters (Author)

No	Constant	Value	Unit
1	E – Young's modulus	124	Gpa
2	ν - Poisson's ratio	0.34	-
3	Density	8960	Kg/m^3
4	A - static yield stress	300	Mpa
5	B - work hardening coefficient	380	Mpa
6	n – work hardening exponent	0.31	-
7	m - thermal softening exponent	1.09	-
8	Melting Temperature	1356	K
9	Transition Temperature	300	K

Figure 8: Johnson-Cook Deformed Profile (Author)

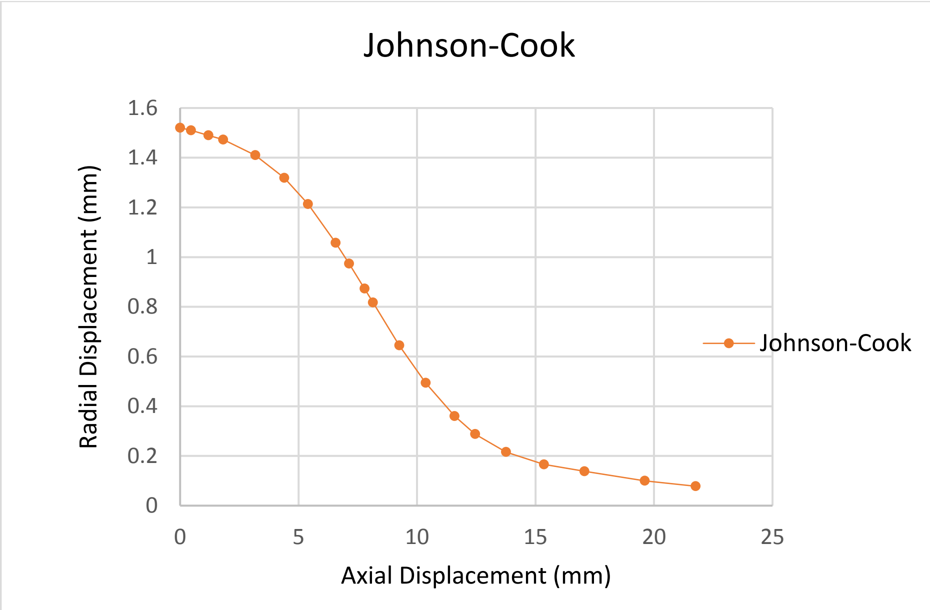

Figure 9: Johnson-Cook Profile Graph with deformation (Author)

2.3 Steinberg-Guinan Plasticity Model

This model is mainly focused and developed for metals suitable at high strain rates and also being further extended for low strain rates. The yield stress increases with the increase in strain rate of the material within a certain limit. It is also proven experimentally that at high pressure, there is no more dependency of rate in materials. As per the experiments, yield stress is a direct function of pressure loaded on material and inversely dependent with the temperature. The model is more focused on effective plastic strain, pressure and temperature.[27]

We have implemented this following model in FEM software for OFHC Cu with following parameters:

Table 4: Steinberg-Guinan Simulation Parameters (Author)

No	Constant	Value	Unit
1	E – Young's modulus	124	Gpa
2	ν - Poisson's ratio	0.34	-
3	Density	8960	Kg/m^3
4	Initial yield stress	300	Mpa
5	Maximum yield stress	640	Mpa

6	B - Hardening constant	36	-
7	n - Hardening exponent	0.45	-
8	Derivative dG/dPG'P	28	-
9	Derivative dG/dTG'T	0.38	PaK-1

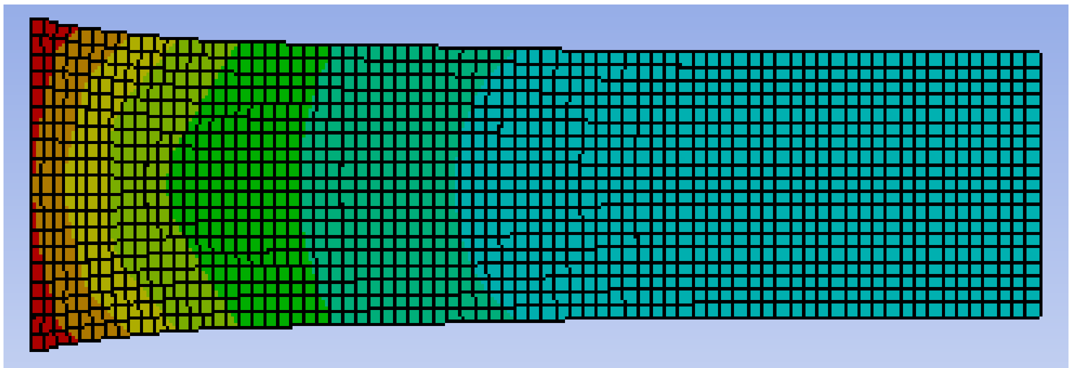

Figure 10: Steinberg-Guinan Deformed Profile (Author)

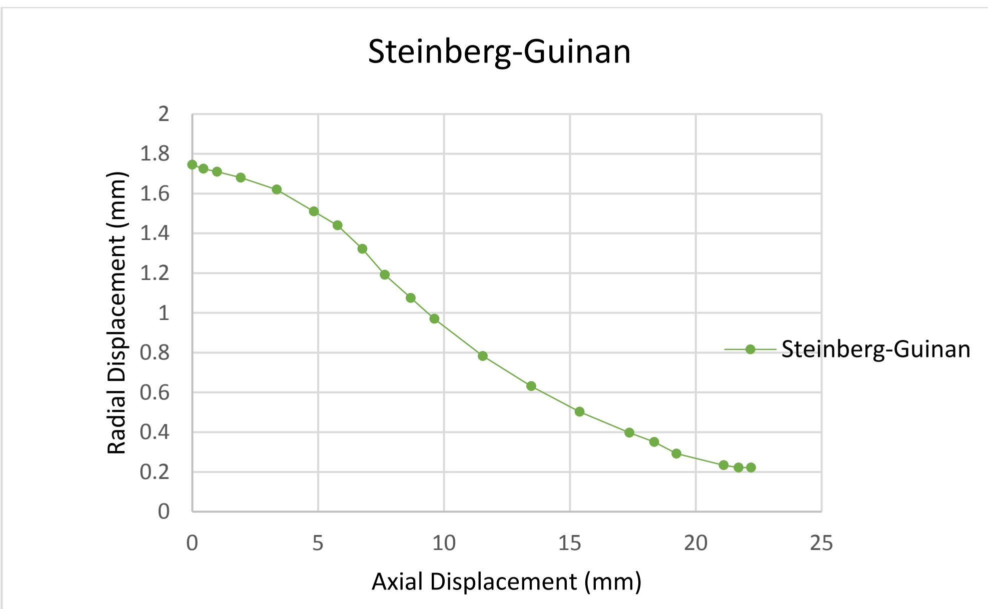

Figure 11: Steinberg-Guinan Profile Graph with deformation (Author)

2.4 Zerilli-Armstrong Plasticity Model

This model is implemented in the same manner as Johnson-Cook model, but it is based on dislocation mechanics. Zerilli-Armstrong model has different types of equation for different materials. Material structure like (BCC, FCC etc.) has their individual constitutive equation based on their rate controlling mechanism [28]. This mechanism solely defined the temperature dependent strain rate effects of different type of materials. The general constitutive equation of this model is based on effective strain hardening, strain rate hardening and thermal softening.

The model is implemented for OFHC – copper in FEM software with the following parameters and results are as followed.

Table 5: Zerilli-Armstrong Material Simulation Parameters (Author)

No	Constant	Value	Unit
1	E – Young's modulus	124	Gpa
2	ν - Poisson's ratio	0.34	-
3	Density	8960	Kg/m^3
4	Initial yield stress	300	Mpa
5	C2 - Zerilli-Armstrong constant	890	Mpa
6	C3 - Zerilli-Armstrong constant	0.0028	K^{-1}
7	C4 - Zerilli-Armstrong constant	0.000115	K^{-1}
8	n - Hardening constant	0.37	-
9	EPS	0.2	-

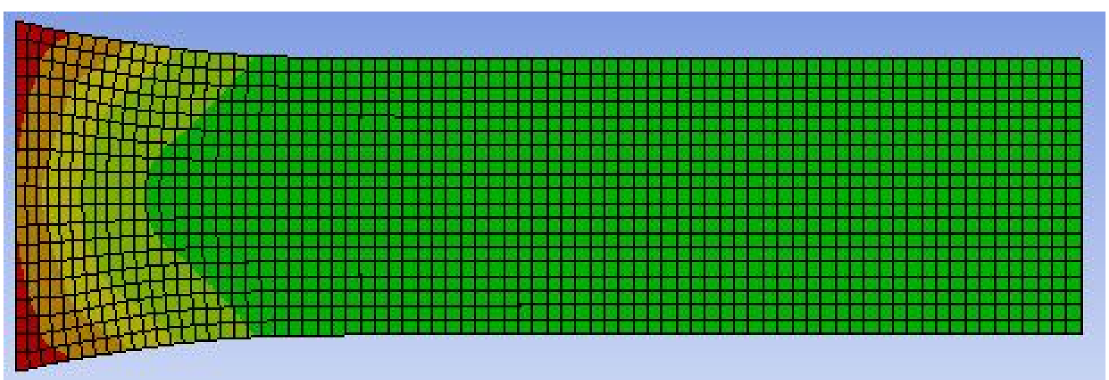

Figure 12: Zerilli-Armstrong Deformed Profile (Author)

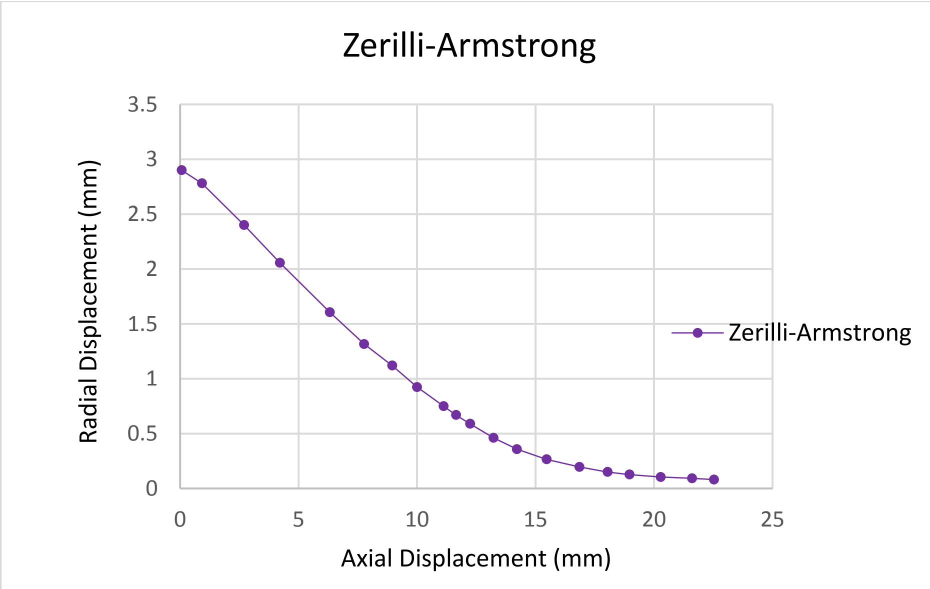

Figure 13: Zerilli-Armstrong Profile Graph with deformation (Author)

2.5 Comparison of results

Table 6: Comparison of conventional models (Author)

S.No	Initial Dimension		Experimental Data		Von-Mises		Johnson-Cook		Steinberg-Guinan		Zerilli-Armstrong	
	Length(L)	Diameter(D)	L	D	L	D	L	D	L	D	L	D
1-	**76.2 (mm)**	**19.05 (mm)**	**71.4 (-4.8) mm**	**23.65 (+4.6) mm**	69.5 (-6.7)	22 (+3.42)	71.1(-5.15)	21.3(+3.01)	70.42(-5.78)	22.70 (+3.49)	69.3(-6.90)	24.85(+5.8)
Error (%)	-	-	-	-	**28.35**	**24.05**	**6.80**	**33.11**	**17.0**	**22.44**	**30.43**	**22.41**

2.6 Summary of Material Models

All conventional models relate the flow stress to the high strain, strain rates and large temperature during impact test. In general material models used in impact testing are grounded on plasticity approach. The von-mises is one of the simplest approaches to acquire dynamic deformation of large strain rates by simply using the plastic stress and strain relation but due to constant constraint the profile evolution and final deformation of sample does not match with experimental data and profile. Among the four conventional model, Johnson-Cook material model is widely used and this model provide the best result among the above discussed models, but once the results are compared with experimental data there is huge percentage of error in lateral displacement that should be taken into account along with reviewing its practical origin and non-coupling with the physical effects, once compared with other plasticity models like Zerilli-Armstrong and Steinberg-Guinan model. As well as model like Zerilli-Armstrong and Steinberg-Guinan model are showing results that are not so much bad in radial direction but if we compare the axial position certainly they have large percentage of error and also both these models are limited for certain identified materials like steel, lead, copper, etc.

CHAPTER 3. FINDINGS - NEW CONSTITUTIVE MODEL

After comparing all the conventional material models in FEM software there seems to be a large percentage of error both in radial and axial directions, which shows that conventional models are unable to predict the exact physics of the process. This needs to be fix by using a new conventional model that is capable of predicting exact physics of the whole process. In this chapter we are going to briefly discuss about the concept behind new model and its implementation to Finite element software (FEM).

From previous known research in this field, the plastic- isotropic hardening material model is a most effective model that can conquer large strain and strain rate hardening in impact test where thermal softening is insignificant. Initially in this chapter we will review this plasticity model and then will make necessary changes so as to achieve our desired new model.

3.1 Hardening

In general, sample gets deformed till yield and then become harden as shown in figure for 1-D case. Perfectly plastic deformation in material is established when the stress is maintained at yield point, once the stress is either dropped or reduced material tends to return to its original shape and size but due to plasticity in material it has some induced strain and this become the hardening case i.e. after yield stress, the stress increases continuously to get plastic deformation. Also, if the stress is constant at any point after the yield point then there will be no more plastic deformation in the material and no elastic unloading.

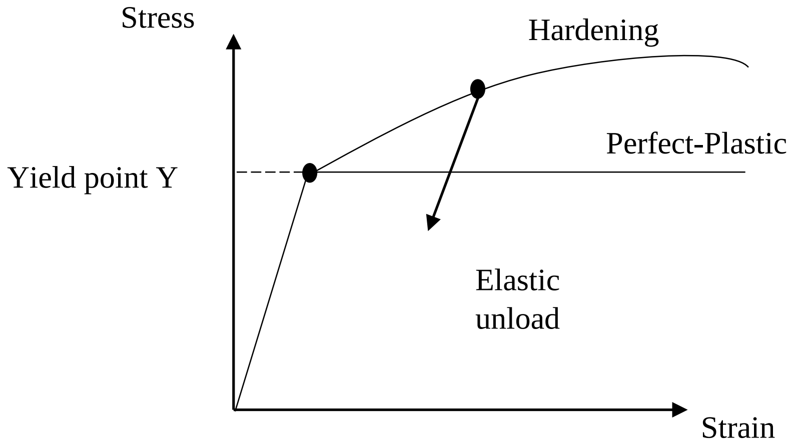

Figure 14: Stress-Strain Curve [2]

The initial yield surface can be written in the form:

$$q_0(\sigma_{ij}) = 0(3.1.1)$$

When, there is perfectly plastic region, the yield surface does not change. For a general case, the formula can be written as:

$$q_0(\sigma_{ij}, J_i) = 0(3.1.2)$$

In the above general formula J_i shows the hardening characteristics of material and used to calculate the change in yield surface. This parameter can be scalar or higher order tensor. At the start of deformation process this parameter is zero.

3.2 Hardening Rule

Generally, there are three rules, but we are going to review isotropic hardening.

3.2.1 Isotropic Hardening

It is the case, when the shape and size increase with the increasing stress without any translation movement.

The yield function is shown as:

$$q_0(\sigma_{ij}, J_i) = q_0(\sigma_{ij}) - J = 0(3.2.1.1)$$

We can conclude from this formula; the shape of yield function depends on the initial yield function and the hardening parameter J which is responsible for the change in size. [29]

The constitutive elasticity equation is as follows:

$$\sigma_{ij} = \lambda\delta_{ij}\varepsilon_{kk}^{el} + 2\mu\varepsilon_{ij}^{el} (3.2.1.2)$$

Integration Procedure

Initially, the von mises stress is calculated and it shows elastic behavior:

$$\overline{\sigma} = \sqrt{\frac{3}{2}G_{ij}G_{ij}}; G_{ij} = G_{ij}^{0} + 2\mu\Delta e_{ij} (3.2.1.3)$$

If the elastic stress is greater than the yield stress, plastic flow starts in the material.

The following equations for stress and plastic strain can be used: [15]

$$\sigma_{ij} = \eta_{ij}\sigma_y + \frac{1}{3}\delta_{ij}\sigma_{kk} (3.2.1.4)$$

$\Delta\varepsilon_{ij} = \frac{3}{2}\eta_{ij}\Delta\overline{\varepsilon}$ where, $\eta_{ij} = G_{ij}/\overline{\sigma}$

The equivalent plastic strain is obtained explicitly through

$\Delta\overline{\varepsilon}^{pl} = \frac{\overline{\sigma}-\sigma_y}{3\mu+h}$; (3.2.1.5) σ_y is the yield stress

$h$is the plastic hardening at the starting.

3.3 Viscoelastic response developed based on Maxwell rheological model

Solid materials show viscoelastic response, this means that they feature intermediate characteristics between purely elastic and purely viscous behavior.

"Viscoelasticity is a property of materials that exhibit time-dependent strain [31]. When deformation in material starts viscoelasticity shows the characteristics between elastic and viscous behavior. Viscous material shows relation of stress with strain rate, simultaneously elastic materials inhibit the direct relation of stress and strain, accounting constant as young's modulus.

Even though most of the developments in the theory of viscoelasticity are recent, the basic linear and isothermal field theory has been available for a much longer time. As we can see there are several contributions by Maxwell, Kelvin and Voigt, the classical theory for linear viscoelasticity was first presented in 1874 by Boltzmann [32]

The behavior of a material may be close to perfectly elastic or viscous that not only depends on strain rate and temperature, but also depends on particular test such as dynamic load testing, ballistic, impact testing, etc. So, as to visualize the response of material, specimen is loaded under dynamic condition, under controlled stress-strain behavior, amplitude of loading and temperature.

If we take a case of perfectly elastic material, the loss of energy during loading and unloading of material is negligible that shows stress and strain are directly proportional to each other, in case of viscous material they are 90º out of phase. In general, material that exhibits this behavior are like metals, polymers, etc.

There exists a complex modulus approach that can define the dynamic behaviour of viscoelastic material [33]. The parameters that characterize viscoelastic properties are dynamic tensile modulus, and the loss tangent. The two components of tensile modulus define the two different characteristics of material i.e. the elastic component count the deformation energy stored by the material and second plastic component measures the loss of energy due to the internal stress generated inside the material after impact, during relaxation process [34].

3.3.1 Stress relaxation:

This is a phenomenon in which the stress in a material reaches a maximum value at time t_0 while maintaining the constant strain and after the stress reaches maximum value it reduces gradually to a minimum value and then it remains constant with time. In this particular test, a strain rate $\dot{\psi}$ is calculated for a γ duration of time then reaches to a maximum value and maintained.

3.3.2 Rheological models.

From the above test, we can determine the material moduli through stress-strain relation and these parameters can be used to get a response of viscoelastic behavior. This can be analyzed while considering mechanical system that demonstrate the response of the material. The mechanical system not only simplify the modelling of material but also at the same time provide us the response of material at high impact loading and accordingly we can understand the stresses generated inside the material.

Basic elements: spring and dashpot

This is a mechanical system consisting of component i.e. Hookean spring and the Newtonian damper [35]. We can define the Hook's law relationship for stress and strain for loading and displacement [36].

$\sigma(t) = \mu\varepsilon(t)$, μ is the modulus of elasticity (3.3.2.1)

The damper is a viscous element and follows Newtonian law for viscosity and represents the component of a viscoelastic material [37].

$\sigma(t) = \eta \frac{\partial\varepsilon}{\partial t}$, η is the viscosity coefficient (3.3.2.2)

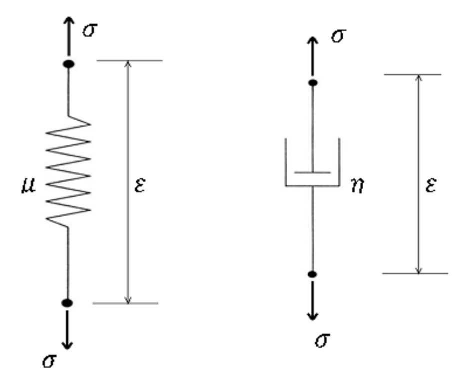

Figure 15: Spring and Dashpot element [38]

Combination of both spring and dashpot elements can be make different models that can describe the response of material.

3.3.3 Maxwell model

In generally this model is a combination of spring and damper in a series arrangement. The total strain on the whole model is summation of strain due to spring element stiffness i.e. μ that changes according to the type of study and load applied to material like Elastic modulus, shear modulus the next part of strain contribution comes from frictional resistance η which is a part of dashpot element. They both follow their individual laws like spring element follows Hooke's law to calculate the stress and strain on the other side the relation is governed by the

Newton's equation for viscous fluid. For this model, the stress remains the same and total strain is given by:

$$\dot{\varepsilon} = \left(\frac{\frac{\partial}{\partial t}}{\mu} + \frac{1}{\eta} \right) \sigma (3.3.3.1)$$

If the material is under a constant strain, the stresses decay gradually.

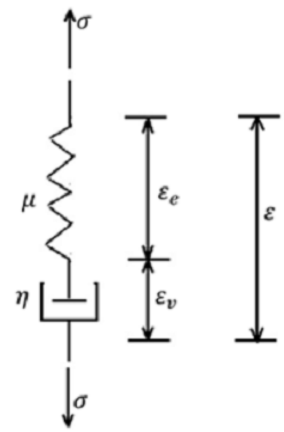

Figure 16: Maxwell Element [38]

3.3.4 Generalized Model

There are mainly different types of generalized models available with different combination of elements but in our thesis, we are stick with single Maxwell element in parallel with the spring element. As in future more elements can be combined to even get much closer results for good qualitative and conceptual analysis. This generalized model with single Maxwell element is known as Zender model [38].

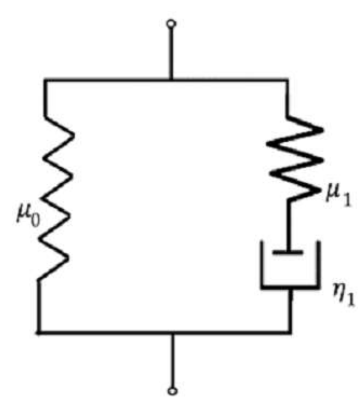

Figure 17: Zener model [38]

The retardation time for this model is the ratio of constant of dashpot element to the constant of spring element:

$$\tau_i = \frac{\eta_i}{\mu_i} \quad (3.3.4.1)$$

3.4 Numerical formulation for linear response (Mathematical Description)

This section is mainly focused on formulation for linear response of a material. This mathematical description is based on a generalized Maxwell rheological model. A one-dimension modeling background for strain of viscoelastic solids is taken. Accordingly, higher order can be proposed [30].

As shown in above figure 4.3., for a single Maxwell element the stress-strain relation is formulated as:

$$\dot{\sigma} + \frac{1}{\tau}\sigma = \mu\dot{\varepsilon} \quad (3.4.1)$$

τ is the relaxation time. Subsequently the homogenous solution for equation (3.4.1):

$$\sigma = C\,exp(-\frac{t}{\tau}) \quad (3.4.2)$$

Constant 'C' can be determined by the initial conditions. Strain 'ε' during the whole relaxation test is constant and below shows the stress response during a period of time 't' and after that it becomes constant. [39]

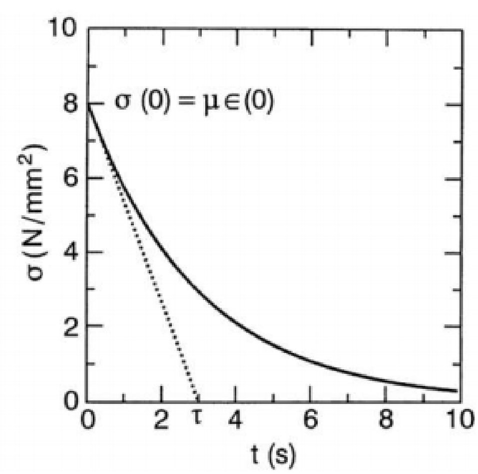

Figure 18: Relaxation test of a Maxwell element [30]

From figure, the initial stress on the material is governed by the elastic response, i.e., at time = 0 the stress on the material $\sigma(0) = \mu\varepsilon(0)$.With this initial condition, constant C in the homogenous solution can be solved. Since the strain in the experiment is constant, i.e., the strain rate is zero, it leads to the particular solution of equation.

If we take a look at the above figure, the initial stress inside the material is due to the elasticity and at time t = 0 the stress is calculated as $\sigma(0) = \mu\varepsilon(0)$ after applying this equation the constant C in the homogenous solution can be resolved. As the strain is constant during the experiment, accordingly the calculated strain rate is zero. Now, so as to calculate the particular solution of equation 3.4.1 taking strain rate to zero is termed as

$$\sigma(t) = \mu\, exp(-\frac{t}{\tau})\varepsilon(0) \text{ (3.4.3)}$$

The relaxation function is termed as

$$\zeta(t) = \mu\, exp(-\frac{t}{\tau}) \text{ (3.4.4)}$$

The above equation indicates the viscoelastic characteristics. The spring constant parallel to the Maxwell elements be μ_0 and the constant for Maxwell elements be μ_1. The viscosity constant of dashpot in the Maxwell element is taken as η_1, we are restriction till one element for more accuracy other elements can be added.

The total stress substitute on the model is equal to the summation of the stresses acting on the spring and the parallel Maxwell elements. The equation of model is expressed as

$$\sigma(t) = \mu_0\varepsilon(0) + \mu_1\, exp(-\frac{t}{\tau_1})\varepsilon(0) \text{ (3.4.5)}$$

τ_1 is the relaxation time for Maxwell element, which is the ratio of viscosity constant of dashpot to the spring constant in Maxwell element. The relaxation function is expressed as

$$\zeta(t) = \mu_0 + \mu_1\, exp(-\frac{t}{\tau_1}) \text{ (3.4.6)}$$

Below equation is the normalized form:

$$\xi(t) = \frac{\zeta(t)}{\mu_0} = 1 + \xi_1\, exp(-\frac{t}{\tau_1}) \text{ (3.4.7)}$$

In the equation (4.4.7) $\xi_1$is the ratio of two spring constantμ_1 toμ_0 . The Cauchy stress for incremental change in strain Δ , is termed as:

$$\sigma(t) = \int_0^t \zeta(t - x) \frac{\partial \varepsilon}{\partial x} dx (3.4.8)$$

The initial response begins at any time x. The relaxation function of material is given as

$$\zeta(t - x) = \mu_0 + \mu_1\, exp(-\frac{t - x}{\tau_1})\ (3.4.9)$$

We can rewrite the (3.4.8) this equation as

$$\sigma(t) = \int_0^t \mu_0 \frac{\partial \varepsilon(x)}{\partial x} dx + \int_0^t \mu_1\, exp(-\frac{(t - x)}{\tau_1}) \frac{\partial \varepsilon(x)}{\partial x} dx\ (3.4.10)$$

Since, $\mu_0$and $\mu_1$is a spring constant and the sum of responses for strain $\partial \varepsilon(x)$ over the time 't' isε (t), equation (3.4.10) is thus revised as

$$\sigma(t) = \mu_0 \varepsilon(t) + \mu_1\, exp(-\frac{(t - x)}{\tau_1}) \varepsilon(t)\ (3.4.11)$$

resulting in

$$\sigma(t) = \sigma_0(t) + I_1(t)\ (3.4.12)$$

Here $\sigma_0(t)$ is the quasi-static stress for the elastic element, and $I_1(t)$ defines the internal stresses in the Maxwell element, i.e.,

$$I_1(t) = \mu_1\, exp(-\frac{(t-x)}{\tau_1}) \sigma(t)\ (3.4.13)$$

From equations (3.4.10) and (3.4.11), and $\varepsilon(x) = \sigma_0(x)/\mu_0$, equation (3.4.13) can be expressed in the other form as $\varepsilon(x) = \sigma_0(x)/\mu_0$, this equation converted into other form as,

$$I_1(t) = \xi_1\, exp(-\frac{(t-x)}{\tau_1}) \sigma(t)\ (3.4.14)$$

Generally, in a relaxation test, the internal stress variable $I_1(t)$ reaches to zero if the time approaches infinity. This shows that when a material is under deformation due to load applied on it, the internal stresses are generated which can be integral part of material during deformation and this stress relax after a certain period of time period $\lim_{t \to \infty} I_1(t) = 0$.

3.5 Implementation of model through VUMAT

In General, Abaqus/Explicit has an interface that allows you to implement constitutive equations. In Abaqus/Explicit the user-defined material model is implemented in user subroutine VUMAT form.

VUMAT is used when there is no existing material model included in Abaqus/Explicit material library so, as to predict the accurate behavior of material that needs to be modelled. By using this user subroutine code, it is possible to define the new constitutive model of different complexity. User-defined material models can be used with Abaqus/Explicit structural element type along with that multiple user materials can be implemented so as to involve all the process during a mathematical modelling. In this section, we will briefly illustrate about how a VUMAT code is implemented inside Abaqus and consequently our new model will be implemented.

A VUMAT code requires proper definition of constitutive equation, particularly in our thesis, we write Cauchy stress equations for large strain applications then defining the proper stress state at the same time it requires classification of dependence on time, field variables, internal state. After writing all the necessary equations it needs to transform into an incremental equation using a suitable integration procedure i.e. implicit, explicit or midpoint method these are then used to update the stresses and dependent state variables.

VUMAT needs following input parameters and defined input procedure in Abaqus.

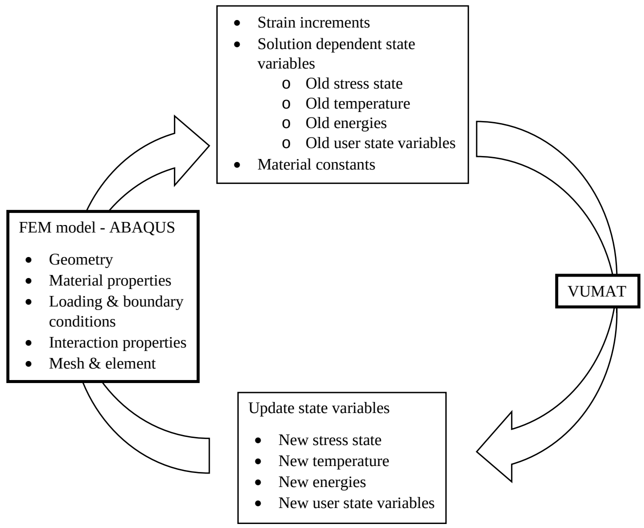

Figure 19: ABAQUS - VUMAT working [15]

To code a particular material model, we should follow the requirement of Abaqus to link Fortran language. As we have used 2017 version of Abaqus to link this version with Fortran, Visual studio 2012 version is linked with Intel parallel studio XE 2016. Once both of this software is downloaded then path of compiler is added to the environment variable of system properties and other linking test like ‘Patch’ test, after that verification of Abaqus is carried out to finally link Fortran language.

After that edit all the material properties that is required like elastic modulus, poison ratio and all the state variables in user material option. The next step is to input FEM model in Abaqus like geometry, mesh and element type, loading conditions, interaction and its properties along with predefined field to add material required velocity.

Once we create a job, we need to link the Fortran .for extension file to a job and the VUMAT file defined material model started with subroutine header that include VUMAT variables like NBLOCK, PROPS, etc. then different conventions are used that shows stress and strain relation and stored as vectors in our case “plane strain and axisymmetric” elements are termed as: s11, s22, s33, s12. Constitutive equation is formulated using stress and strain which yields the same results with any plastic option in general model without VUMAT.

In our model the necessary updates are carried out with yield stress. So, as to implement and investigate the internal stresses generated in the material, we take into account the new model in VUMAT and results for our model is true for large-strain calculations. As Abaqus uses Newton's method to solve equation. So, our implemented code uses the same method so that the accuracy doubles after each step of iteration.

3.6 Results

After implementing the new VUMAT code in Abaqus results are shown as a deformed profile, along with a chart showing change in axial and radial position.

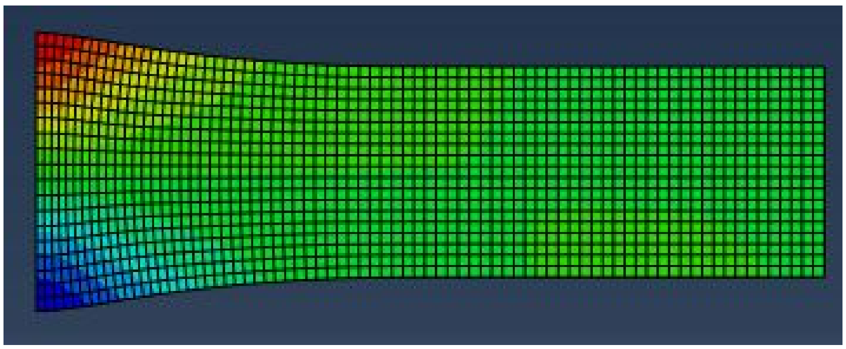

Figure 20: New model deformed profile (Author)

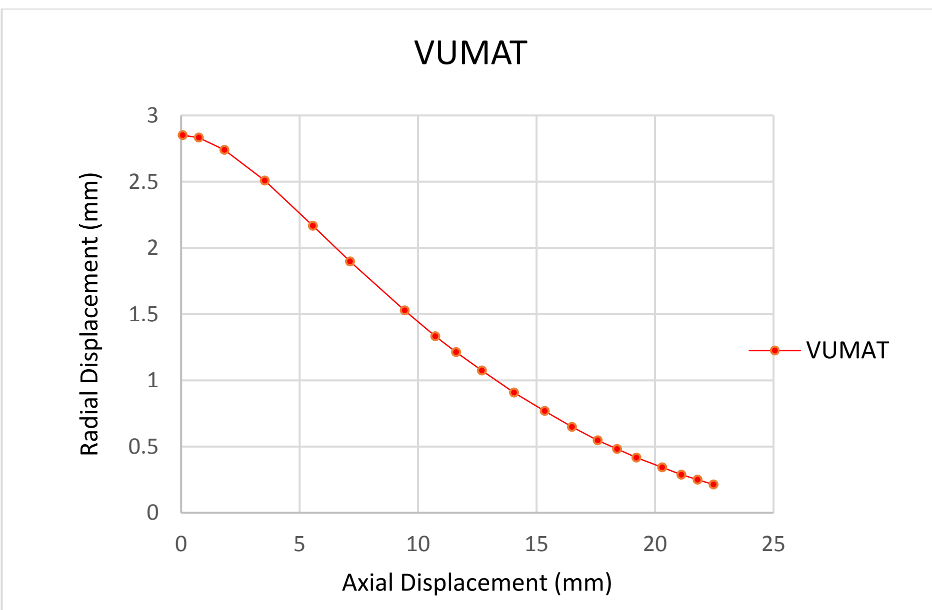

Figure 21: New model profile graph with deformation (Author)

CHAPTER 4. RESULTS - MODEL COMPARISON AND PROFILE EVALUATION

In this chapter all the plasticity models' results are discussed in a tabular format so, as to know which plasticity model predicts the best result once compared with the experimental data.

Table 7: Final comparison of all plasticity models (Author)

Initial Dimensions	**Experimental Results**	**Deformed Profile Results**	**Error(%)**
von Mises Approach			
Length (mm) 76.2	71.4 (-4.8)	69.5 (-6.7)	28.35
Diameter(mm) 19.05	23.55 (+4.5)	22.65 (+3.4)	24.05
Johnson Cook Approach			
Length (mm) 76.2	71.4 (-4.8)	71.05 (-5.15)	6.80
Diameter(mm) 19.05	23.55 (+4.5)	22.06 (+3.01)	33.11
Zerilli Armstrong			
Length (mm) 76.2	71.4 (-4.8)	69.3 (-6.90)	30.43
Diameter(mm) 19.05	23.55 (+4.5)	24.85 (+5.8)	22.41
Steinberg Guinan			
Length (mm) 76.2	71.4 (-4.8)	70.42(-5.78)	17.00
Diameter(mm) 19.05	23.55 (+4.5)	22.70(+3.49)	22.44
New Model (VUMAT)			
Length (mm) 76.2	71.4 (-4.8)	71.2(-5.0)	4.00
Diameter(mm) 19.05	23.55 (+4.5)	24.71(+5.66)	20.49

Profile Evaluation:

In the below, there are charts to compare the different material model profile with the experimental profile [4]. The profiles are compared at different impact timings so as to get the exact physics of problem.

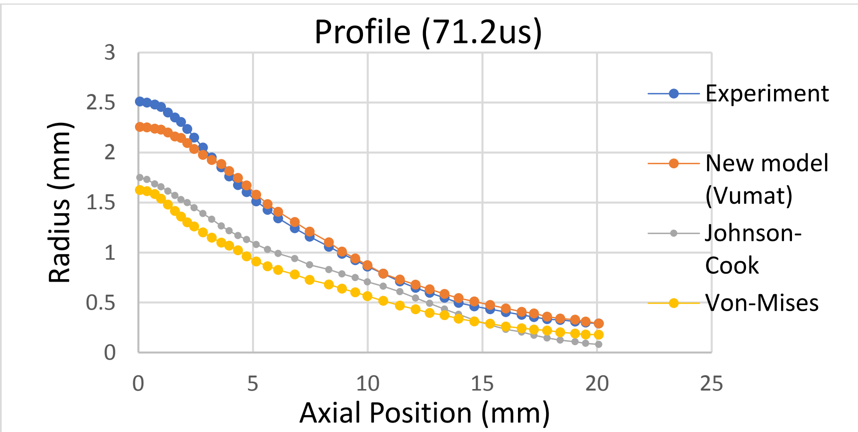

Figure 22: Material models comparison at 71.2µs [4, Author]

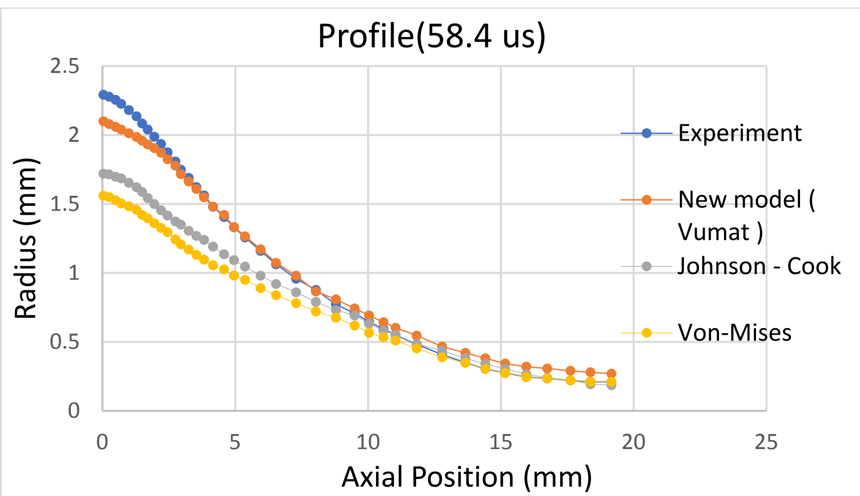

Figure 23: Material models comparison at 58.4µs [4, Author]

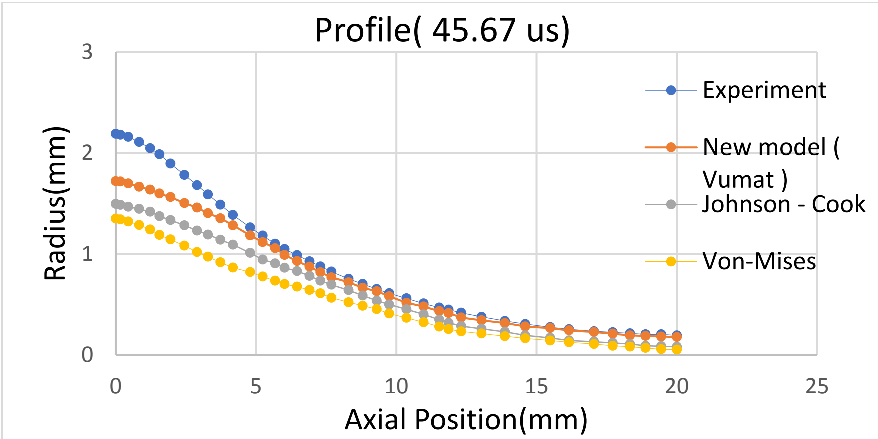

Figure 24: Material models comparison at 45.67µs [4, Author]

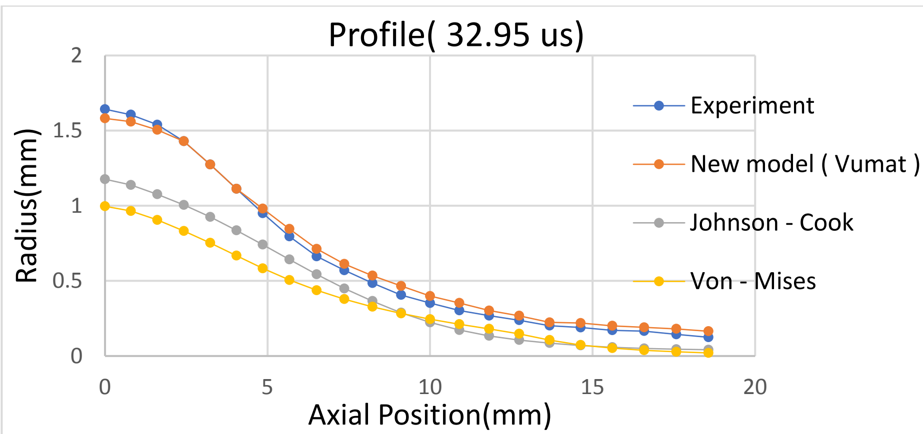

Figure 25: Material models comparison at 32.95µs [4, Author]

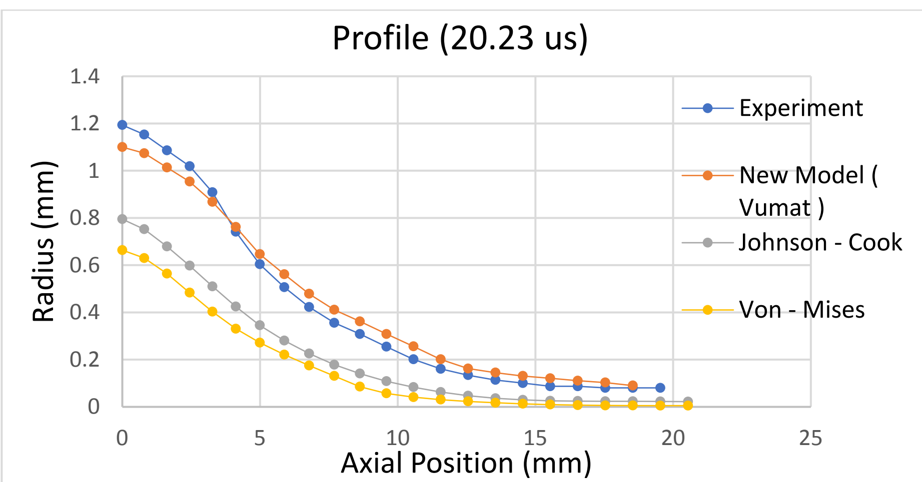

Figure 26: Material models comparison at 32.95µs [4, Author]

CHAPTER 5. CONCLUSION AND RECOMMENDATION

Different plasticity models are discussed like Von-Mises [26], Johnson Cook [25], Steinberg Guinan [23] and Zerilli Armstrong [24] in the literature review after a brief background and understanding of these models in Chapter 2 all the conventional models are implemented through Finite element software like Abaqus, Ansys. The conventional models are performed numerically at 83 m/s using Taylor rod-on-anvil impact test along with all conventional models are provided with same yield stress and their particular constant parameter.

After that in the same chapter, conventional models deformed profile and results are discussed with experimentally performed results [4]. A comparison is conducted, and it is concluded that Johnson-Cook provides the best result for axial displacement once compare with the experimental data and at the same time Steinberg Guinan provides the good predictability of radial displacement of rod(specimen) at low velocity but deformation in radial and axial deformation was with a large percentage of error. Other models like Zerilli Armstrong and Von-Mises models shows a large percentage of error on both sides.

Chapter 3 shows the implementation of new model as all the conventional models shows a large percentage of error either in both radial and axial displacement or in single direction. This model is aimed to focus to get the exactness of FEM results with experimental data, so more enforcement is done to know about the dynamic yielding of process. The new model follows the change in yield stress due to the internal stresses generated inside the material using a viscoelastic response of material.

After presenting all the background and mathematical description, new material model is implemented as VUMAT (user-defined material model) in Abaqus 2017 a general-purpose FEM software, coding of user-defined model is carried out in a by default language of Abaqus i.e. Fortran. After applying this code in Abaqus, results and verification of this model are compared with the experimental data and other conventional models and it illustrate that outcomes are far better than all other discussed conventional models, it is seen that the percentage of error in axial direction is reduced from the largest of 30% to 4% and for radial direction error reduces from maximum 33% to 20%.

For furthermore validation of results, transient deformation of states at different impact timings are compared for selected conventional model, new implemented model with experimental data [4]. It is clearly shown in (Figure: 22,23,24,25,26) that implemented new model shows good prediction of transient states of deformation as well as from table (Table: 7) good prediction of final deformed state of impacted samples at 83 m/s if compared with conventional models.

This thesis has laid the groundwork for further research into significance and behavior of material models for high strain, high strain rates and temperature simulations. There are certainly some open areas where more enhancement of new model can be implemented i.e. implementing a greater number of Maxwell elements so as to get better results in radial direction and second recommendation to consider the micro mechanisms of plastic deformation and the defect structure evolution as that changes with strain rate increase i.e. implementation of structure parameter such as grain size.

REFERENCES

[1] Dannemann, Kathryn & Chalivendra, Vijaya & Song, Bo. (2012). Dynamic Behavior of Materials. Experimental Mechanics. 52. 10.1007/s11340-012-9598-0.

[2] "Yield surface," Wikipedia. March. 20, 2020, Accessed: March. 20, 2020. [Online]. Available: https://en.wikipedia.org/w/index.php?title=Yield_surface&oldid=960994049.

[3] Wilkins, M.L., Guinan, M.W., 1973. Impact of cylinders on a rigid boundary. Journal of Applied Physics. 44, №3, 1200 – 1206

[4] Eakins, D.E., Thadhani, N.N., 2006. Instrumented Taylor anvil-on-rod impact tests for validating applicability of standard strength models to transient deformation states. Journal of Applied Physics 100, 073503.

[5] Hill, R., "The Mathematical Theory of Plasticity", Clarendon Press (reprint), 1998.

[6] Kachanov, L.M., "Fundamentals of the Theory of Plasticity", Dover Publications, 2004.

[7] Khan, A.S. and Huang, S., "Continuum Theory of Plasticity", John Wiley and Sons, 1995.

[8] Mises, R.V., "Mechanik der plastischen Formanderung von Kristallen", Zeitschrift für Angewandte Mathematik und Mechanik, 8, 161–185, 1928.

[9] "Constitutive equation," Wikipedia. March. 22, 2020, Accessed: March. 22, 2020. [Online]. Available: https://en.wikipedia.org/wiki/Constitutive_equation

[10] Encyclopaedia of Physics (2nd Edition), R.G. Lerner, G.L. Trigg, VHC publishers, 1991, ISBN (Verlagsgesellschaft) 3-527-26954-1, ISBN (VHC Inc.) 0-89573-752-3

[11] "Cauchy stress tensor," Wikipedia. March. 22, 2020, Accessed: March. 22, 2020. [Online].https://en.wikipedia.org/wiki/Cauchy_stress_tensor

[12] Hearn E. J.: Mechanics of Materials, Volume 1. Second Edition, Pergamon Press, 1985, pp 1 - 4.

[13] Stouffer D. C. and Dame L. T: Inelastic Deformation of Metals. John Wiley & Sons Inc., 1996, general reference.

[14] Lubliner J.: Plasticity Theory. Macmillan Publishing Company, 1990, pp 69 - 82.

[15] Hibbitt, Karlsson and Sorensen: ABAQUS Theory Manual. ABAQUS 6.3-1 Documentation, 2002.

[16] Hearn E. J.: Mechanics of Materials, Volume 1. Second Edition, Pergamon Press, 1985, pp 1 - 4.

[17] Thomson R: Plastic constitutive theory, part 2: plastic flow. http://www.mech . gla.ac.uk/~rthomson/teaching/lecnotes/ch30 . Htm

[18] Mendelson A.: Plasticity: Theory and Application. The Macmillan Company, 1968, general reference.

[19] Gronostajski Z.: The constitutive equations for FEM analysis. J. Mat. Proc. Tech., 106, 2000, pp 40 - 44.

[20] Bai Y. and Dodd B.: Adiabatic shear localization. Pergamon Press, 1992, pp 104 -129.

[21] Steinberg, D.J.; Lund, C.M. (1988), "A constitutive model for strain rates from 10−4 to 106 s−1", Journal de Physique. Colloques, 49 (3): 3, retrieved 2009-05-13

[22] “Isotropic Hardening - an overview | ScienceDirect Topics.” https://www.sciencedirect.com/topics/engineering/isotropic-hardening (accessed Feb. 06, 2020).

[23] Steinberg, D.J., Cochran, S.G., Guinan, M.W., 1980. A constitutive model for metals applicable at high strain rates. J. Appl. Phys., 51, 1498–1504.

[24] Zerilli F. J. and Armstrong R. W.: Dislocation - mechanics - based constitutive relations for material dynamics calculations.J. AppI. Phys. 61(5), March 1987, pp 1816 - 1825.

[25] Johnson, G.R., Cook, W.H.,1983. A constitutive model and data for metals subjected to large strains, high strain rates and high temperatures. Proc.of 7th Symposium on Ballistics (Netherlands, Hague) p 541

[26] "Von Mises Criterion (Maximum Distortion Energy Criterion)". Engineer's edge. Retrieved 8 February 2018.

[27] Applied Impact Mechanics: C. Lakshmana Rao, V. Narayanamurthy, K. R. Y. Simha John Wiley & Sons Pg- 147-154

[28] Liang R and Khan A.S.: A critical review of experimental results and constitutive models for Bee and Fee metals over a wide range of strain rates and temperatures. IntI. J. Plasticity, 15, 1999, pp 963 - 980.

[29] “Springer Handbook of Experimental Solid Mechanics - Google Books.” https://books.google.ru/books?id=I_1y1OkqZqQC&pg=PA92&lpg=PA92&dq=29.+Solid+Mechanics+Part+II+303+by+Kelly&source=bl&ots=FjBfbC9D_P&sig=ACfU3U30mLyZRw_IWozi4ZprIO85bU8oxA&hl=en&sa=X&ved=2ahUKEwiEt_6kuu3pAhXyh4sKHeIJD_cQ6AEwAHoECAgQAQ#v=onepage&q=29.%20Solid%20Mechanics%20Part%20II%20303%20by%20Kelly&f=false (accessed Feb. 06, 2020).

[30] Gillani, Asim, "Development Of Material Model Subroutines For Linear And Nonlinear Response Of Elastomers" (2018). Electronic Thesis and Dissertation Repository. 5837. https://ir.lib.uwo.ca/etd/5837.

[31] Meyers, M.A., and Chawla, K.K., "Mechanical Behavior of Materials," Cambridge University Press, Cambridge, UK, 2009,

[32] M. G. Ianniello and G. Israel, “Boltzmann’s ‘Nachwirkung’ and Hereditary Mechanics,”pp. 1–31.

[33] Rao, M.D., "Recent applications of viscoelastic damping for noise control in automobiles and commercial airplanes," Journal of Sound and Vibration, Vol. 262, No. 3, 2003, pp. 457-474.

[34] Nowick, A.S., and Berry, B.S., "Anelastic relaxation in crystalline solids," Academic Press, New York; London, 1972, pp. 677.

[35] S. P. C. Marques and G. J. Creus, Computational viscoelasticity, no. 9783642253102. 2012.

[36] Z. Martinec, “Continuum Mechanics,” Time, p. 179, 2011.

[37] D. S. Viswanath, T. K. Ghosh, D. H. L. Prasad, N. V. K. Dutt, and K. Y. Rani, “Theories of Viscosity,” in Viscosity of Liquids: Theory, Estimation, Experiment, and Data, 2007, pp. 109–133.

[38] R. Xiao, H. Sun, and W. Chen, “An equivalence between generalized Maxwell model and fractional Zener model,” Mech. Mater., vol. 100, pp. 148–153, 2016.

[39] M. Kaliske and H. Rothert, “Formulation and implementation of three-dimensional viscoelasticity at small and finite strains,” Comput. Mech., vol. 19, no. 3, pp. 228–239, 1997.

[40] L. Schwer, “Optional Strain-Rate Forms for the Johnson Cook Constitutive Model and the Role of the Parameter Epsilon_0,” p. 17.

[41] Taylor G.I.: The use of flat-ended projectiles for determining dynamic yield stress: I. Theoretical considerations. Proc. Roy. Soc. Lon., Vol. 194,1948, pp 289 - 299.

[42] Taylor G.I.: The use of flat-ended projectiles for determining dynamic yield stress: II. Tests on various metals. Proc. Roy. Soc. Lon., Vol. 194, 1948, pp 300 - 322.

[43] Wilkins M.L. and Guinan M.W.: Impact of cylinders on a rigid boundary. J. Appl. Phys., Vol. 44, No.3, 1973, pp 1200 -1206.

[44] Kapoor Rand Nemat-Nasser S.: Determination of temperature rise during high strain rate deformation.